Copyright © 2015 Tech Science Press CMES, vol.107, no.3, pp.223-247, 2015

An Explicit Time Marching Technique With Solution-Adaptive Time Integration Parameters

Delfim Soares Jr.[1]

Abstract: In this work, an explicit time marching procedure, with solution-adaptive time integration parameters, is introduced for the analysis of hyperbolic models. The proposed technique is conditionally-stable, second-order accurate and it has controllable algorithm dissipation, which locally adapts at each time step, according to the computed solution. Thus, spurious modes can be more effectively dissipated and accuracy is improved. Since this is an explicit time integration technique, the new procedure is very efficient, requiring no system of equations to be dealt with at each time-step. Moreover, the technique is simple and easy to implement, being based just on displacement-velocity relations, requiring no computation of accelerations. Numerical results are presented along the paper, illustrating the good performance of the new method, as well as its potentialities.

Keywords: Time integration methods; Explicit analysis; Adaptive parameters; Adaptive dissipation control; Stability; Accuracy.

1 Introduction

In the literature, an adaptive time marching technique is usually referred to as a mechanism that interactively proposes changes to the time step employed in the analysis, in order to achieve a desired level of accuracy. In this sense, several works have been proposed along the last decades, being several procedures available nowadays [Choi and Chung (1996); Logg (2004); Lages, Silveira, Cintra, and Frery (2013) etc. – for a recent overview on the topic, the work of Rossi, Ferreira, Mansur, and Calenzani (2014), is referred]. Adaptive time stepping is not the focus here. In this work, time integration parameters are adaptively computed, taking into account different spatial and temporal distributions.

The concept of adaptive time integration parameters is also not new (e.g., Soares, (2014; 2015a, b)); however, in most works, this is carried out just once, in the

[1] Structural Engineering Department, Federal University of Juiz de Fora, CEP 36036-330, Juiz de Fora, MG, Brazil. Email: delfim.soares@ufjf.edu.br

beginning of the analysis, taking into account the physical and geometrical proprieties of the model. In fact, explicit-implicit time marching techniques can be regarded as a special case of this simplified approach, where "stiffer" subdomains (which may arise from locally refined spatial discretizations, heterogeneous material distributions etc.) are treated by implicit integrators, whereas the more "flexible" subdomains are treated by explicit time integration parameters [Miranda, Ferencz, and Hughes (1989); Gravouil and Combescure (2001)].

Here, a full adaptive strategy is considered, i.e., not only different values for the time integrators may be considered along the spatial domain of the model, but also they may vary along the time domain, adapting themselves according to the evolution of the computed solution. In addition, the proposed adaptive strategy is non-iterative, being the new values for the time integrators directly computed taking into account just previous time-step results. Thus, the present technique is quite generic and efficient.

The main goal here is to adapt the time integration parameters in order to properly dissipate spurious modes, providing more accurate analyses. Numerous efforts during the past decades have focused on developing time integration algorithms that include controllable numerical dissipation and improved accuracy [Hilbert *et al*., (1977); Hulbert and Chung (1996); Chow and Kim (2002); Leontyev (2010); Soares (2011); Idesman (2011) etc.]. The purpose of numerical dissipation is to reduce spurious, non-physical oscillations that sometimes occur due to excitation of spatially unresolved modes. One basic difficulty in designing such dissipative algorithms is to add high-frequency dissipation without introducing excessive algorithmic damping in the important low-frequency modes. Thus, in the present technique, the time integrators are adaptively computed, introducing algorithm dissipation into the analysis only when it is necessary. This is carried out based on a local oscillatory criterion, being dissipative elements locally activated once oscillations occur in the computed solution. When no oscillatory behavior is observed, non-dissipative time integrators are employed. As it is well known, the central difference method (CDM), which is the nearly universal choice once explicit time integration is considered, possesses no numerical dissipation. Thus, the technique cannot deal with spurious modes, and non-physical oscillations may occur in the solutions computed using the CDM. The present adaptive method acts extinguishing these spurious oscillations once they arise.

The paper is organized as follows: first, the governing equations of the model and the time integration strategy are presented, describing how the adaptive computation of the time integration parameters is carried out. In the sequence, the properties of the proposed methodology are discussed, and numerical applications are presented, illustrating the good performance of the new technique, as well as its po-

tentialities. As one will observe, the proposed approach is second-order accurate, simple to implement, and quite effective to dissipate high-frequency modes and to accurately compute low-frequency answers. An extra positive feature that arises in the proposed formulation, is the fact that the technique is only based on single-step displacements-velocities relations. Thus, the technique is truly self-starting, eliminating any kind of cumbersome initial procedure, such as the computation of initial accelerations and/or the computation of multistep initial values.

2 Governing equations and time integration strategy

The governing system of equations describing a linear dynamic model is given by [Clough and Penzien (1993)]:

$$\mathbf{M}\ddot{\mathbf{U}}(t)+\mathbf{C}\dot{\mathbf{U}}(t)+\mathbf{K}\mathbf{U}(t)=\mathbf{F}(t) \tag{1}$$

where $\mathbf{M}$, $\mathbf{C}$ and $\mathbf{K}$ are mass, damping and stiffness matrices, respectively, $\mathbf{F}(t)$ stands for the force vector and $\mathbf{U}(t),\dot{\mathbf{U}}(t)$ and $\ddot{\mathbf{U}}(t)$ are displacement, velocity and acceleration vectors, respectively. The initial conditions of the model are given by:

$$\mathbf{U}^0=\mathbf{U}(0) \tag{2a}$$

$$\dot{\mathbf{U}}^0=\dot{\mathbf{U}}(0) \tag{2b}$$

where $\mathbf{U}^0$ and $\dot{\mathbf{U}}^0$ stand for initial displacement and velocity vectors, respectively.

By time integrating equation (1) at the element level (element variables are here indicated by e), considering a time-step Δt, one may write:

$$\mathbf{M}_e\int_{t-\frac{\Delta t}{2}}^{t+\frac{\Delta t}{2}}\ddot{\mathbf{U}}_e(\tau)d\tau+\mathbf{C}_e\int_{t-\frac{\Delta t}{2}}^{t+\frac{\Delta t}{2}}\dot{\mathbf{U}}_e(\tau)d\tau+\mathbf{K}_e\int_{t-\frac{\Delta t}{2}}^{t+\frac{\Delta t}{2}}\mathbf{U}_e(\tau)d\tau=\int_{t-\frac{\Delta t}{2}}^{t+\frac{\Delta t}{2}}\mathbf{F}_e(\tau)d\tau \tag{3}$$

which may be viewed as a simple weighted residual form of the local equations of motion.

The integrals in the l.h.s. of equation (3) may be approximated by:

$$\Im_{\ddot{\mathbf{U}}_e}^{n+\frac{1}{2}}=\int_{t-\frac{\Delta t}{2}}^{t+\frac{\Delta t}{2}}\ddot{\mathbf{U}}_e(\tau)d\tau\approx\dot{\mathbf{U}}_e^{n+1}-\dot{\mathbf{U}}_e^n \tag{4a}$$

$$\Im_{\dot{\mathbf{U}}_e}^{n+\frac{1}{2}}=\int_{t-\frac{\Delta t}{2}}^{t+\frac{\Delta t}{2}}\dot{\mathbf{U}}_e(\tau)d\tau\approx\mathbf{U}_e^{n+1}-\mathbf{U}_e^n \tag{4b}$$

$$\Im_{\mathbf{U}_e}^{n+\frac{1}{2}}=\int_{t-\frac{\Delta t}{2}}^{t+\frac{\Delta t}{2}}\mathbf{U}_e(\tau)d\tau\approx\Delta t\mathbf{U}_e^n+\frac{1}{2}\alpha_e^n\Delta t^2\dot{\mathbf{U}}_e^n \tag{4c}$$

where $\mathbf{U}^n$, $\dot{\mathbf{U}}^n$ and $\ddot{\mathbf{U}}^n$ are the approximations of $\mathbf{U}(t^n)$, $\dot{\mathbf{U}}(t^n)$ and $\ddot{\mathbf{U}}(t^n)$, respectively, $t^n = n\Delta t$, and α_e^n is the time integration parameter of the new method, computed at each element and at each time step. The displacement $\mathbf{U}^{n+1}$ can be defined by the following simple finite difference expression:

$$\mathbf{U}^{n+1} = \mathbf{U}^n + \frac{1}{2}\Delta t\dot{\mathbf{U}}^n + \frac{1}{2}\Delta t\dot{\mathbf{U}}^{n+1} \tag{5}$$

Taking into account approximations (4) and (5), equation (3) may be rewritten as the following recursive relation:

$$(\mathbf{M}_e + \frac{1}{2}\Delta t\mathbf{C}_e)\dot{\mathbf{U}}_e^{n+1} = \Im_{\mathbf{F}_e}^{n+\frac{1}{2}} + \mathbf{M}_e\dot{\mathbf{U}}_e^n - \frac{1}{2}\Delta t\mathbf{C}_e\dot{\mathbf{U}}_e^n - \mathbf{K}_e(\Delta t\mathbf{U}_e^n + \frac{1}{2}\alpha_e^n\Delta t^2\dot{\mathbf{U}}_e^n) \tag{6}$$

where $\Im_{\mathbf{F}_e}^{n+\frac{1}{2}}$ stands for the integral in the r.h.s. of equation (3).

As it can be observed, when $\mathbf{M}$ and $\mathbf{C}$ are diagonal, the method is explicit. Once assembling is considered, equation (6) enables to compute the velocities $\dot{\mathbf{U}}^{n+1}$, and equation (5) may then be used to compute the displacements at the current time step. It is important to highlight that the method described by equations (5) and (6) is a single-step method based only on velocities and displacements, being no computation of accelerations required. Thus, the first positive feature of the method is that it is truly self-starting, eliminating any kind of cumbersome initial procedure, such as the computation of initial accelerations (which usually requires an extra system of equations to be dealt with) and/or the computation of multistep initial values.

As it may be observed in equations (4c) and (6), different α parameters may be selected for each element and for each time step. Thus, a spatial/temporal adaptive procedure may be developed, locally computing the time integration parameter α according to the evolution of the computed fields. This is carried out here based on an oscillatory criterion. In this sense, if the computed response of a degree of freedom of the model oscillates along time, the α parameters of the elements surrounding this degree of freedom are modified, locally introducing numerical dissipation into the analysis. Once no oscillatory behavior is observed, the α parameters are kept unitary (as it is discussed in the next section, for $\alpha = 1$, no amplification decay is introduced into the analysis).

The above idea can be mathematically established as follows: (i) for each time step and for each element, compute an oscillatory parameter φ_e^n, as described in equation (7) (in this equation, η_e stands for the total amount of degrees of freedom of the element); (ii) if this oscillatory parameter is null, no degree of freedom of the element is oscillating along time, and $\alpha_e^n = 1$ is considered (equation (8a)), introducing no numerical dissipation into the analysis; (iii) if this oscillatory parameter

is not null, at least one degree of freedom of the element is oscillating, and $\alpha_e^n > 1$ is considered (equation (8b)), introducing numerical dissipation into the analysis.

$$\varphi_e^n = \sum_{i=1}^{\eta_e} \left(\left| u_i^n - u_i^{n-2} \right| - \left| u_i^n - u_i^{n-1} \right| - \left| u_i^{n-1} - u_i^{n-2} \right| \right) \tag{7}$$

$$\text{If } \varphi_e^n = 0, \alpha_e^n = 1 \tag{8a}$$

$$\text{If } \varphi_e^n \neq 0, \alpha_e^n = 1 + a\omega\Delta t \tag{8b}$$

In equation (8b), a stands as an input control parameter and ω represents an estimation for the highest natural frequency of the model. The intensity of the algorithm dissipation is proportional to a and, for $a = 0$, no numerical damping is introduced. As indicated by equations (5)–(8), the proposed time integration method is an efficient and simple to implement technique, based on a single parameter a, which controls the dissipative intensity of the method.

The oscillatory criterion represented by equation (7) indicates if an oscillation occurs taking into account the computed results at the last three time steps. Following this simple criterion, if the solution increment within two consecutive time steps (i.e., $|u^n - u^{n-2}|$) is not equal to the sum of the corresponding increments within one time step (i.e., $|u^n - u^{n-1}| + |u^{n-1} - u^{n-2}|$), an oscillation occurs.

In the next section, the properties of the described time marching technique are analyzed, and expressions (8) are further discussed.

3 Properties of the method

In this section, the single degree of freedom (SDOF) problem is considered in order to discuss the properties (i.e., stability, accuracy etc.) of the proposed methodology, following standard guidelines. The equation of motion for the SDOF model can be written as:

$$\ddot{u}(t) + 2\xi w\dot{a}u(t) + w^2 u(t) = f(t) \tag{9}$$

where ξ is the damping ratio and w is the natural frequency of the model. Considering equation (9) and the proposed methodology, the following recursive relationship can be written:

$$\begin{bmatrix} u^{n+1} \\ \dot{u}^{n+1} \end{bmatrix} = \begin{bmatrix} A_{11} & A_{12} \\ A_{21} & A_{22} \end{bmatrix} \begin{bmatrix} u^n \\ \dot{u}^n \end{bmatrix} + \begin{bmatrix} L_{11} & L_{12} & L_{13} \\ L_{21} & L_{22} & L_{23} \end{bmatrix} \begin{bmatrix} f^n \\ f^{n+\frac{1}{2}} \\ f^{n+1} \end{bmatrix} = \mathbf{A} \begin{bmatrix} u^n \\ \dot{u}^n \end{bmatrix} + \mathbf{L} \begin{bmatrix} f^n \\ f^{n+\frac{1}{2}} \\ f^{n+1} \end{bmatrix} \tag{10}$$

where $\mathbf{A}$ and $\mathbf{L}$ stand for the amplification and the load operator matrices, respectively.

In the proposed technique, the amplification matrix **A** is given by equations (11):

$$A_{11} = [1 + \xi w\Delta t - \frac{1}{2}w^2\Delta t^2]/A_0 \tag{11a}$$

$$A_{12} = [1 - \frac{1}{4}\alpha w^2\Delta t^2]\Delta t/A_0 \tag{11b}$$

$$A_{21} = [-w^2\Delta t^2](1/\Delta t)/A_0 \tag{11c}$$

$$A_{22} = [1 - \xi w\Delta t - \frac{1}{2}\alpha w^2\Delta t^2]/A_0 \tag{11d}$$

where $A_0 = 1 + \xi w\Delta t$.

The load operator matrix **L** may be given by:

$$L_{11} = \frac{1}{2}\beta_1\Delta t^2/A_0 \tag{12a}$$

$$L_{12} = \frac{1}{2}\beta_2\Delta t^2/A_0 \tag{12b}$$

$$L_{13} = \frac{1}{2}\beta_3\Delta t^2/A_0 \tag{12c}$$

$$L_{21} = \beta_1\Delta t/A_0 \tag{12d}$$

$$L_{22} = \beta_2\Delta t/A_0 \tag{12e}$$

$$L_{23} = \beta_3\Delta t/A_0 \tag{12f}$$

where β_1, β_2 and β_3 are integration parameters. These parameters can be selected, for instance, as $\beta_1 = \beta_3 = 1/4$ and $\beta_2 = 1/2$, if the trapezoidal quadrature rule is followed, or as $\beta_1 = \beta_3 = 1/6$ and $\beta_2 = 2/3$, if the Simpson rule is followed. If linear behaviour is assumed for the load within Δt, the load integration parameters can be simply selected as $\beta_1 = \beta_3 = 1/2$ and $\beta_2 = 0$.

In the proposed technique, different α values are expected to simultaneously occur in the analysis, as well as time varying values are supposed to occur. Therefore, in this section, the properties of the technique are discussed considering different values for α, in order to illustrate a basic range of features that may develop (locally in space and time) once the proposed methodology is applied.

3.1 Convergence

The expansion of the amplification matrix of the new method in Taylor's series, considering expressions (8), is given by:

$$A_{11} = 1 - \frac{1}{2}w^2\Delta t^2 + \frac{1}{2}\xi w^3\Delta t^3 - \frac{1}{2}\xi^2 w^4\Delta t^4 + \frac{1}{2}\xi^3 w^5\Delta t^5 + O(\Delta t^6) \tag{13a}$$

$$A_{12} = \Delta t - \xi w \Delta t^2 - (\frac{1}{4} - \xi^2) w^2 \Delta t^3 - (\frac{1}{4}\frac{\omega}{w} a - \frac{1}{4}\xi + \xi^3) w^3 \Delta t^4 + \\ + (\frac{1}{4}\frac{\omega}{w} a\xi - \frac{1}{4}\xi^2 + \xi^4) w^4 \Delta t^5 + O(\Delta t^6) \tag{13b}$$

$$A_{21} = -w^2 \Delta t + \xi w^3 \Delta t^2 - \xi^2 w^4 \Delta t^3 + \xi^3 w^5 \Delta t^4 - \xi^4 w^6 \Delta t^5 + O(\Delta t^6) \tag{13c}$$

$$A_{22} = 1 - 2\xi w \Delta t - (\frac{1}{2} - 2\xi^2) w^2 \Delta t^2 - (\frac{1}{2}\frac{\omega}{w} a - \frac{1}{2}\xi + 2\xi^3) w^3 \Delta t^3 + \\ + (\frac{1}{2}\frac{\omega}{w} a\xi - \frac{1}{2}\xi^2 + 2\xi^4) w^4 \Delta t^4 \\ - (\frac{1}{2}\frac{\omega}{w} a\xi^2 - \frac{1}{2}\xi^3 + 2\xi^5) w^5 \Delta t^5 + O(\Delta t^6) \tag{13d}$$

By comparing it with the expansion of the analytical amplification matrix, which is given by:

$$A^a_{11} = 1 - \frac{1}{2} w^2 \Delta t^2 + \frac{1}{3}\xi w^3 \Delta t^3 + \frac{1}{24}(1 - 4\xi^2) w^4 \Delta t^4 \\ - \frac{1}{30}(\xi - 2\xi^3) w^5 \Delta t^5 + O(\Delta t^6) \tag{14a}$$

$$A^a_{12} = \Delta t - \xi w \Delta t^2 - \frac{1}{6}(1 - 4\xi^2) w^2 \Delta t^3 + \frac{1}{6}(\xi - 2\xi^3) w^3 \Delta t^4 + \\ + \frac{1}{10}(\frac{1}{12} - \xi^2 + \frac{4}{3}\xi^4) w^4 \Delta t^5 + O(\Delta t^6) \tag{14b}$$

$$A^a_{21} = -w^2 \Delta t + \xi w^3 \Delta t^2 + \frac{1}{6}(1 - 4\xi^2) w^4 \Delta t^3 - \frac{1}{6}(\xi - 2\xi^3) w^5 \Delta t^4 + \\ - \frac{1}{10}(\frac{1}{12} - \xi^2 + \frac{4}{3}\xi^4) w^6 \Delta t^5 + O(\Delta t^6) \tag{14c}$$

$$A^a_{22} = 1 - 2\xi w \Delta t - \frac{1}{2}(1 - 4\xi^2) w^2 \Delta t^2 + \frac{2}{3}(\xi - 2\xi^3) w^3 \Delta t^3 + \\ + \frac{1}{24}(1 - 12\xi^2 + 16\xi^4) w^4 \Delta t^4 \\ - \frac{1}{60}(3\xi - 16\xi^3 + 16\xi^5) w^5 \Delta t^5 + O(\Delta t^6) \tag{14d}$$

one may observe that the method is second-order accurate, independently of a and ω.

3.2 Stability and numerical dissipation

The stability condition requires that matrix $\mathbf{A}$ does not amplify errors as the time-step algorithm advances on time. The conditions required to assure stability are [Hughes (2000); Bathe (1996)]: (i) $\rho(\mathbf{A}) \leq 1$; (ii) eigenvalues of $\mathbf{A}$ of multiplicity greater than one are strictly less than one in modulus. In item (i), $\rho(\mathbf{A})$ is the

spectral radius of matrix **A**, which represents the maximal absolute magnitude of the eigenvalues of **A**.

The eigenvalues of the amplification matrix of the proposed method are given by equation (15), where A_1 is half the trace of matrix **A** and A_2 is the determinant of **A**, as defined by equations (16):

$$\lambda_{1,2}(\mathbf{A}) = A_1 \pm (A_1^2 - A_2)^{1/2} \tag{15}$$

$$A_1 = [1 - \frac{1}{4}(\alpha+1)\Omega^2]/A_0 \tag{16a}$$

$$A_2 = [1 - \xi\Omega + \frac{1}{2}(1-\alpha)\Omega^2]/A_0 \tag{16b}$$

where $\Omega = w\Delta t$ is the sampling frequency of the model.

By analyzing the spectral radius of matrix **A**, it can be established that the method is conditionally stable if $\alpha \geq 1$ and unconditionally unstable if $\alpha < 1$. For $\alpha = 1$, several features of the central difference method are reproduced, including the spectral radius behavior. For $\alpha > 1$, numerical damping is introduced into the algorithm. The critical sampling frequency Ω_c, which is the value of Ω under which stability is assured, is given by:

$$\Omega_c = 2\alpha^{-1/2} \tag{17}$$

and, for Ω_c, the spectral radius is $\rho_c = 1$.

Because the higher modes of semidiscrete equations are artifacts of the discretization process and not representative of the behaviour of the governing partial differential equations, it is generally viewed as desirable and often is considered absolutely necessary to have some form of algorithmic damping present to remove the participation of the high-frequency modal components [Hughes (2000)]. Maximization of high-frequency dissipation is obtained by restricting the eigenvalues of the amplification matrix to be complex conjugate, i.e., by requiring that $A_1^2 < A_2$. In this case, the bifurcation sampling frequency Ω_b, which is the value of Ω at which complex conjugate eigenvalues bifurcate into real, distinct eigenvalues, is given by:

$$\Omega_b = 4(\alpha+1)^{-1} \tag{18}$$

At the bifurcation sampling frequency, the spectral radius achieves a minimal value, which is given by $\rho_b = |\alpha-3|/|\alpha+1|$. Thus, for $\alpha = 3$, $\rho = 0$ at $\Omega = 1$. In Fig.1, the spectral radii of the proposed method are depicted for various values of α. In Fig.2, a scheme is presented, illustrating the main characteristics of the spectral radius as function of α.

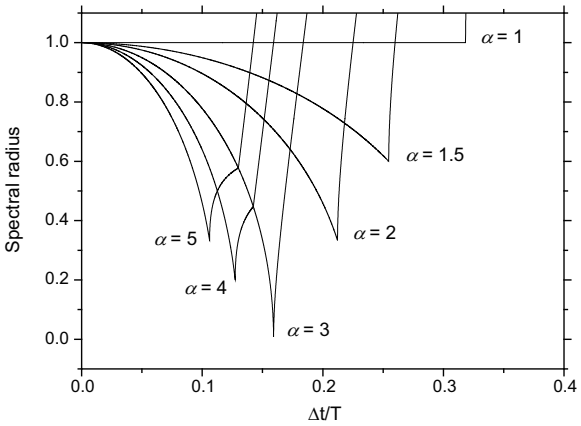

Figure 1: Spectral radii.

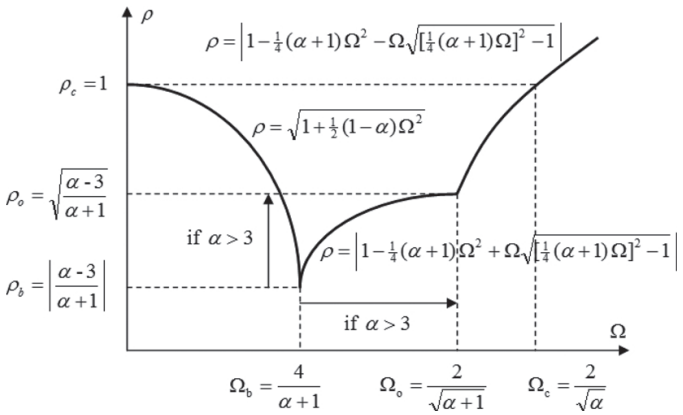

Figure 2: Spectral radius behaviour.

3.3 Accuracy

Taking into account the homogeneous SDOF model equation, velocities may be eliminated by repeated use of (10) to obtain a difference equation in terms of displacements, as follows:

$$u^{n+1} - 2A_1 u^n + A_2 u^{n-1} = 0 \tag{19}$$

Comparison of (19) with the characteristic equation of **A** indicates that the solution has the representation:

$$u^n = c_1 \lambda_1^n + c_2 \lambda_2^n \tag{20}$$

where the coefficients c_1 and c_2 are determined by the initial data and it is considered that $\lambda_1 \neq \lambda_2$. When λ_1 and λ_2 are complex conjugate, solution (20) can be

compared to the undercritically-damped model solution

$$\bar{u}^n = \exp(-\bar{\xi}\bar{w}t^n)[\bar{c}_1\cos(\bar{w}_D t^n) + \bar{c}_2\sin(\bar{w}_D t^n)] \tag{21}$$

allowing to establish error measures.

Considering $\lambda_{1,2} = A \pm Bi$, $c_{1,2} = c_r \pm c_i i$ and $\bar{c}_{1,2} = \bar{c}_r \pm \bar{c}_i i$, the comparison of equations (20) and (21) provides:

$$(c_r \pm c_i i)(A \pm Bi)^n = (\bar{c}_r \pm \bar{c}_i i)\exp[(-\bar{\xi}\bar{w} \pm \bar{w}_D i)\Delta t n] \tag{22}$$

where:

$$c_r = \bar{c}_r = \frac{1}{2}u^0 \tag{23a}$$

$$c_i = \frac{1}{2}[(A - A_{11})/B]u^0 - \frac{1}{2}[A_{12}/B]\dot{u}^0 \tag{23b}$$

$$\bar{c}_i = \frac{1}{2}[-\xi w/w_D]u^0 - \frac{1}{2}[1/w_D]\dot{u}^0 \tag{23c}$$

By adopting the polar forms $A \pm Bi = \rho\exp(\pm\phi i)$, $c_r \pm c_i i = r\exp(\pm\theta i)$ and $\bar{c}_r \pm \bar{c}_i i = \bar{r}\exp(\pm\bar{\theta} i)$, equation (22) can be rewritten as:

$$(r/\bar{r})\rho^n \exp[(\pm\phi n \pm \theta \mp \bar{\theta})i] = \exp(-\bar{\xi}\bar{w}\Delta t n)\exp[(\pm\bar{w}_D\Delta t n)i] \tag{24}$$

from which one may define:

$$\bar{w}_D\Delta t = \phi + (\theta - \bar{\theta})/n \tag{25a}$$

$$\bar{\xi}\bar{w}\Delta t = -\ln(\rho) \tag{25b}$$

$$A_f = (r/\bar{r})^{1/n} \tag{25c}$$

which allows to compute period elongation, amplitude decay and amplitude factor error measures, respectively [Soares (2015a)]. In Fig.3, $(w/\bar{w}-1)$, $\bar{\xi}$ and A_f are depicted, considering the standard undamped unitary initial displacement model and some values of α (one should keep in mind that for $\alpha = 1$, the basic features of the central difference method are reproduced).

4 Numerical applications

In this section, two numerical examples are considered, illustrating the performance and potentialities of the proposed adaptive technique. First, the transversal motion of a square membrane is studied and, in the sequence, an acoustic fluid layer is analyzed. The computed results are compared to those of the central difference

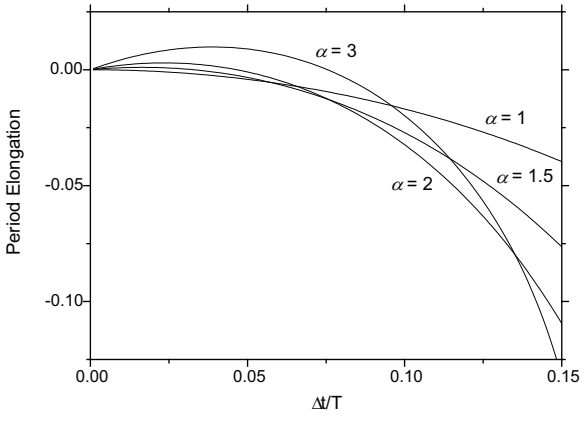

(a)

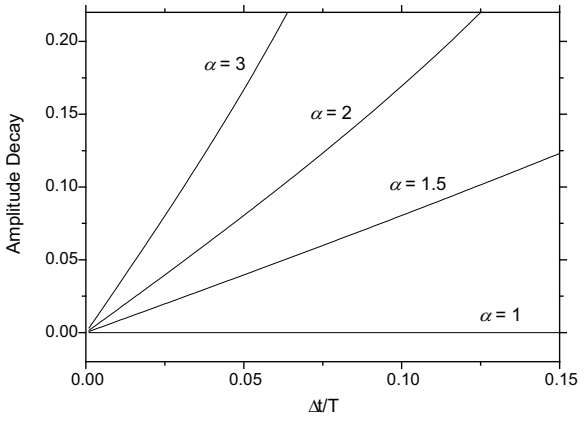

(b)

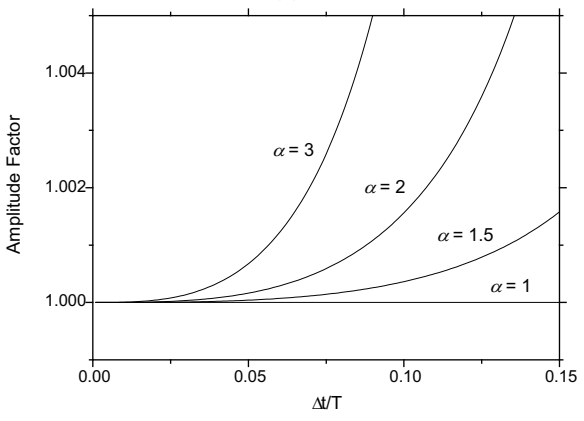

(c)

Figure 3: Period elongation (a), amplitude decay (b) and amplitude factor (c).

method and to analytical answers. In the analyses that follow, linear triangular finite elements are employed for the spatial discretization. A measure of the adopted time-step length is computed according to the following expression:

$$\gamma = c\Delta t/\ell \tag{26}$$

where c is the (primary) wave velocity and ℓ is the characteristic finite element length.

4.1 Application 1

The subject of this investigation is the transverse motion of a square membrane that has initial velocity prescribed over its central domain (grey area in the sketch of Fig.4) and null displacements prescribed over its entire boundary (Mansur *et al.*, 2007). The physical properties of the membrane are $c = 10$ m/s (wave velocity) and $\rho = 1$ kg/m^3 (mass density). The geometry of the model is defined by $L = 10$ m and $l = 0.4$ m. The symmetry of the membrane is considered and just 1/4 of it is discretized. Two spatial/temporal discretizations are considered here, namely: (i) "discretization 1", considering 5000 finite elements and $\Delta t = 0.0025$s; and (ii) "discretization 2", considering 20000 finite elements and $\Delta t = 0.00125$s. Both discretizations provide $\gamma \approx 0.25$.

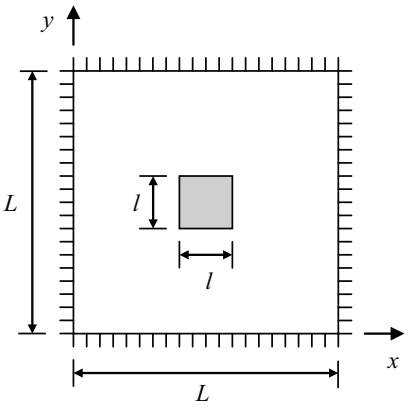

Figure 4: Sketch of the membrane.

The analytical solution for the transversal displacement of the membrane is given by:

$$u_A(x,y,t) = \frac{4Lv_0}{c\pi^3} \sum_{m=1}^{\infty} \sum_{n=1}^{\infty} \frac{C_{mn}}{mn(m^2+n^2)^{1/2}} \sin\left(\frac{m}{L}\pi x\right) \sin\left(\frac{n}{L}\pi y\right) \sin\left(\frac{(m^2+n^2)^{1/2}}{L}\pi ct\right) \tag{27}$$

where $C_{mn} = [\cos(c_1 m) - \cos(c_2 m)][\cos(c_1 n) - \cos(c_2 n)]$, $c_1 = \frac{\pi}{2}(1 + l/L)$, $c_2 = \frac{\pi}{2}(1 - l/L)$ and v_0 stands for the amplitude of the applied initial velocity.

Analytical answers are depicted in Fig.5, taking into account the discretized domain of the membrane and four time instants, namely: $t = 0.75$s, $t = 1.50$s, $t = 2.00$s and $t = 2.50$s. Results provided by the CDM are also depicted in the figure, considering discretizations 1 and 2. As it can be observed in Fig.5, spurious modes are not dissipated by the CDM, drastically damaging the quality of the computed results.

In Figs 6 and 7, results considering the proposed technique are presented, considering discretizations 1 and 2, respectively. As it is illustrated in the figures, the new technique provides much better results than the CDM, properly dissipating the spurious modes of the model. In fact, taking into account discretization 2, very good results are obtained, being the computed solutions depicted in Fig.7 very close to the analytical answers for the membrane. It is important to highlight that, despite the geometrical simplicity of the membrane, the present application represents a rather complex time-domain numerical computation. Here, successive reflections occur at the model extremities and these systematic multiple reflections can emphasize some numerical deficiencies, such as numerical instabilities, excessive numerical damping and/or errors amplifications. As it can be observed, the proposed technique deals very properly with this complex numerical model.

In Figs 6 and 7, the evolutions of the time integration parameters along space and time are also illustrated. In these figures, the elements with non-unitary α values are marked, indicating the active dissipative elements at the focused time instants. As one can notice, just few dissipative elements, properly distributed along space and time, are able to eliminate the influence of spurious high frequency modes, barely damaging the solution of the lower modes.

In Fig.8, time history results at the middle of the membrane are depicted, taking into account the aforementioned procedures and discretizations. Fig.8 highlights once more the good performance of the proposed methodology: the new technique allows to extinguish spurious oscillations without introducing excessive errors into the analysis. In Tab.1, the obtained relative errors (L2 norm) of the new technique and of the CDM are provided, considering the focused analyses. As it can be observed, the proposed technique provides lower errors for all the considered cases.

The influence of spurious modes is more visually remarkable taking into account variables based on the spatial derivatives of the main computed field (as gradients, stresses etc.). In Fig.9, the gradient evolution of the computed field is depicted, considering a location point close to the middle of the membrane (i.e., at the center of the boundary edge of the closest finite element). As one can observe, in this case, the CDM provides very inaccurate results once it is unable to deal with spurious

(a) (b) (c)

(d) (e) (f)

(g) (h) (i)

(j) (k) (l)

Figure 5: Computed fields at different instants of time: 1st column – analytical answer; 2nd column – CDM (discretization 1); 3rd column – CDM (discretization 2); 1st row – t = 0.75s; 2nd row – t = 1.50s; 3rd row – t = 2.00s; 4th row – t = 2.50s.

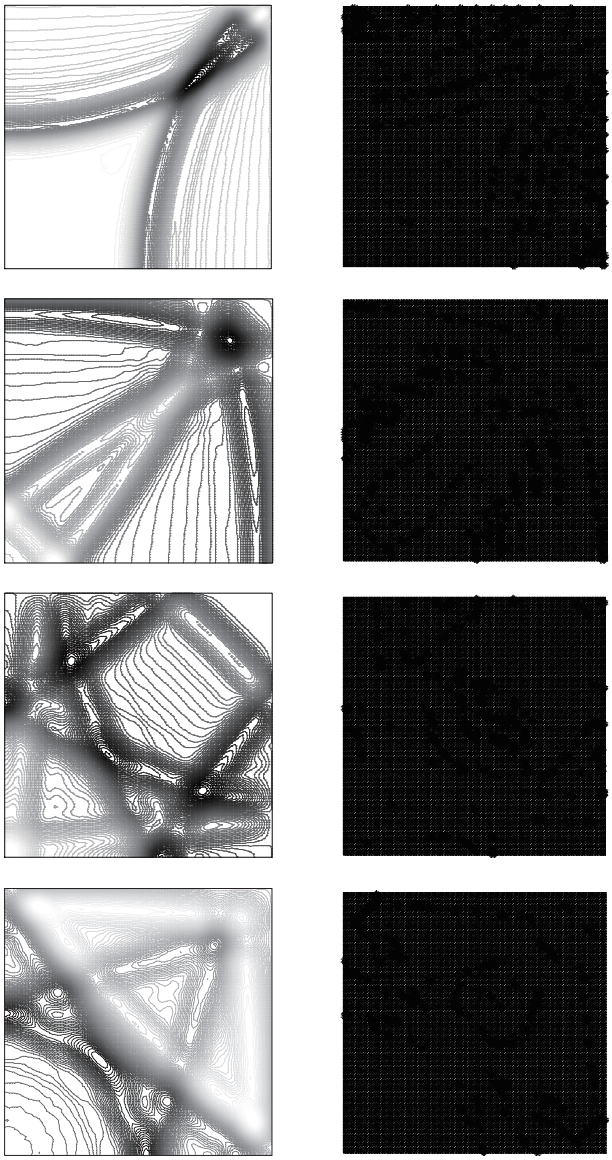

Figure 7: Computed fields and dissipative elements (marked by '*') at different instants of time considering the new technique ($a = 3$) and discretization 2: 1st row – $t = 0.75s$; 2nd row – $t = 1.50s$; 3rd row – $t = 2.00s$; 4th row – $t = 2.50s$.

4.2 Application 2

A strip of an acoustic fluid is considered here, as described in Fig.10. The height of the fluid layer is defined by $L = 2$ m. The physical properties of the model are

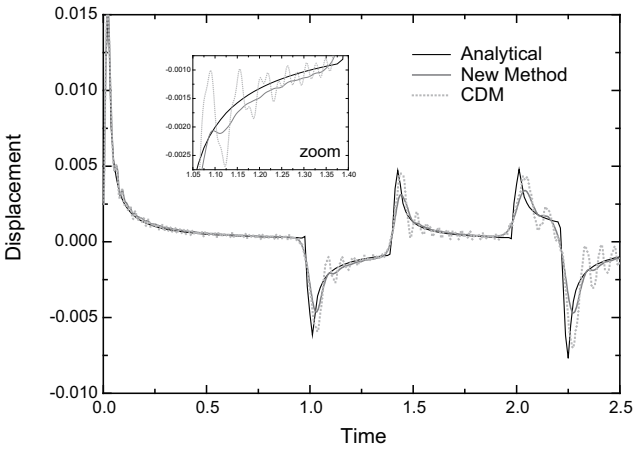

(a) discretization 1

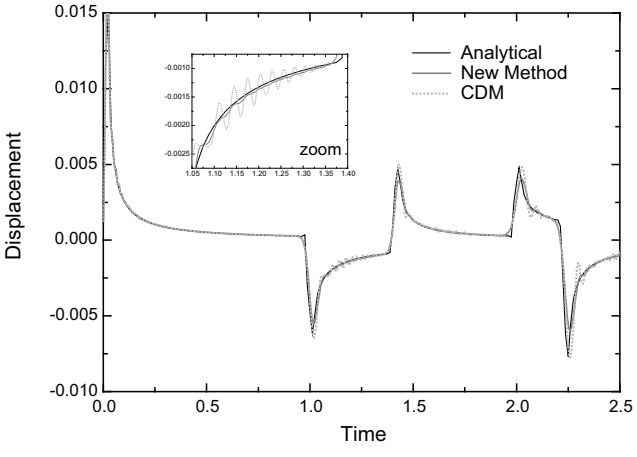

(b) discretization 2

Figure 8: Time history results at the middle of the membrane considering different procedures.

Table 1: Computed relative errors.

Method	Discretization	Membrane	Fluid Layer
CDM	1	0.319	0.039
	2	0.163	0.024
New	1	0.282	0.033
	2	0.156	0.021

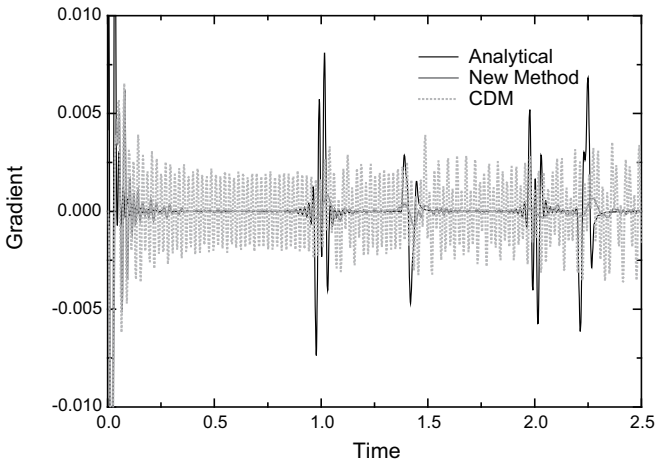

Figure 9: Time history results at $0.05m$ (horizontal distance) of the middle of the membrane considering different procedures (discretization 1).

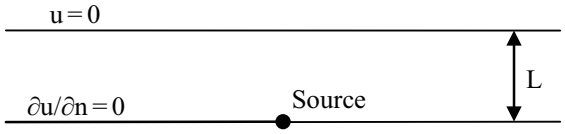

Figure 10: Sketch of the fluid layer.

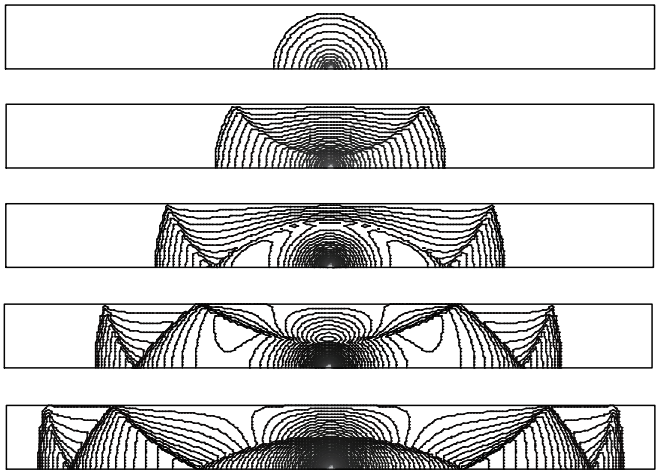

Figure 11: Evolution of the computed fields at each $0.0012s$ – analytical answer.

$c = 1500$ m/s (wave velocity) and $\rho = 1000$ kg/m^3 (mass density). Null Dirichlet

and Newman boundary conditions are prescribed over the top and the bottom of the strip, respectively. A point source is applied at the bottom of the fluid layer, acting invariably along time (Heavised time behaviour). As in the previous application, two spatial/temporal discretizations are considered here, namely: (i) "discretization 1", considering 8000 finite elements and $\Delta t = 2 \cdot 10^{-5}$s; and (ii) "discretization 2", considering 32000 finite elements and $\Delta t = 10^{-5}$s. Both discretizations provide $\gamma \approx 0.30$.

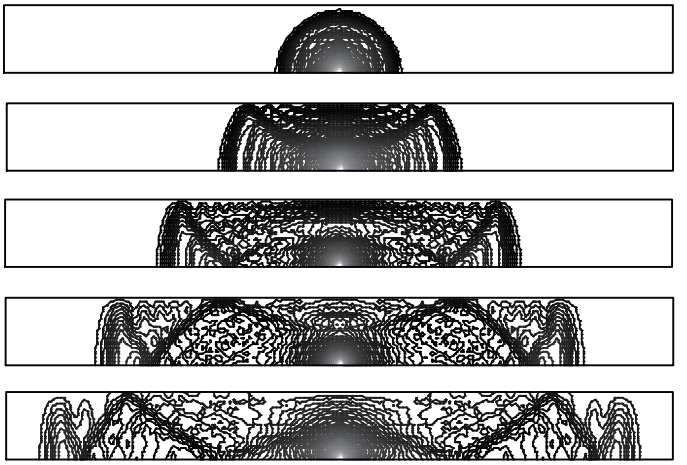

(a) discretization 1

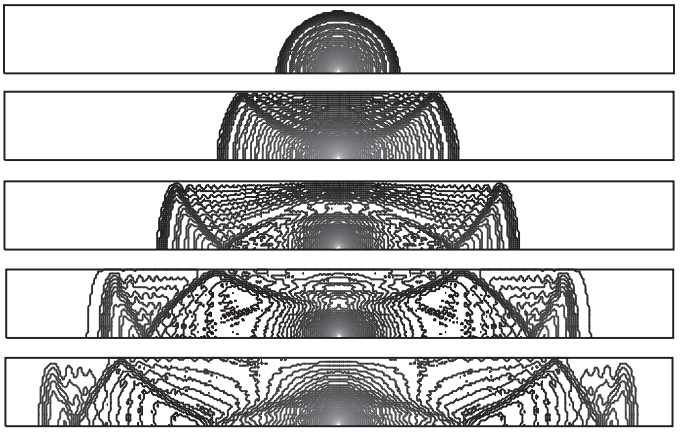

(b) discretization 2

Figure 12: Evolution of the computed fields at each $0.0012s$ – CDM.

For this model, analytical answers can be derived taking into the account the solu-

tion related to a constant point source acting at an infinite medium:

$$u_A(d,t) = \frac{A}{2\pi\rho c^2} \ln\left(\frac{ct + (c^2t^2 - d^2)^{1/2}}{d}\right) H(ct-d) \tag{28}$$

In equation (28), d is the distance between the source and the field points, H stands for the Heaviside function and A is the amplitude of the applied source. Once solutions of the form (28) are superposed, taking into account multiple "ghost" reflected sources, the analytical solution for the present model can be obtained.

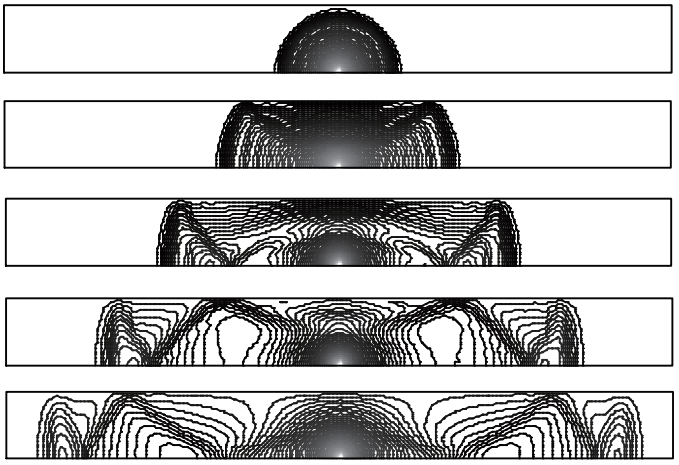

(a) discretization 1

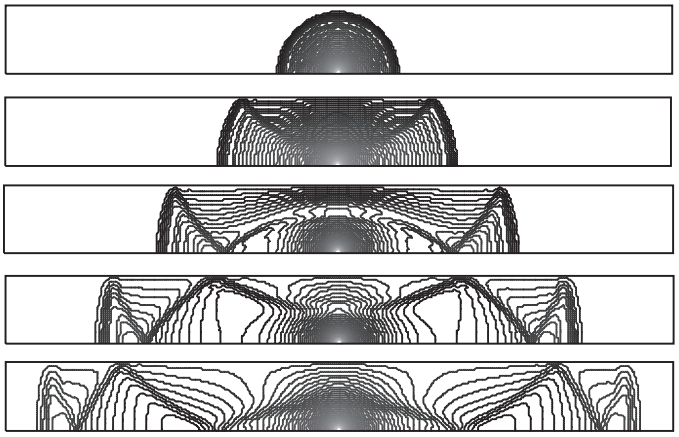

(b) discretization 2

Figure 13: Evolution of the computed fields at each $0.0012s$ – new method ($a = 3$).

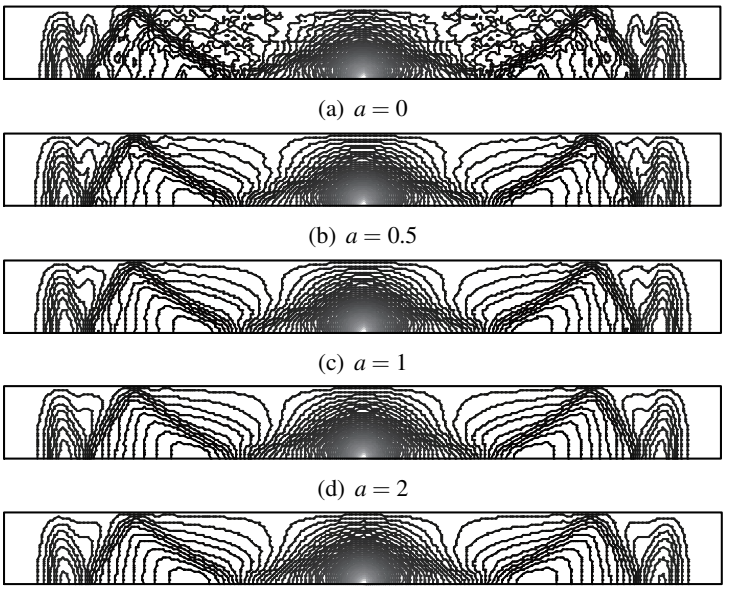

(a) $a = 0$

(b) $a = 0.5$

(c) $a = 1$

(d) $a = 2$

(e) $a = 3$

Figure 14: Computed fields at $t = 0.006s$ considering the new method (discretization 1).

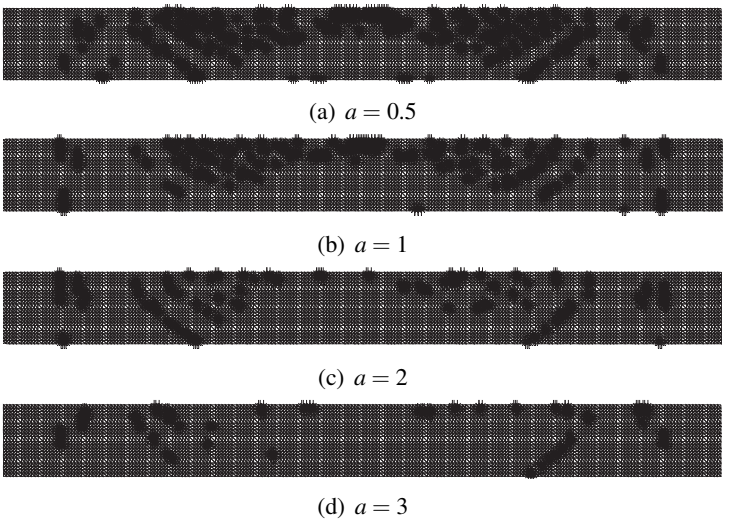

(a) $a = 0.5$

(b) $a = 1$

(c) $a = 2$

(d) $a = 3$

Figure 15: Dissipative elements at $t = 0.006s$ considering the new method (discretization 1).

In Figs.11, 12 and 13, results computed along the discretized strip are depicted, considering the analytical solution, the CDM and the new method, respectively. As one can observe, once again the new technique provides good results. As it is illustrated in the figures, the new technique properly dissipates the spurious modes of the model, rendering better results than the standard CDM.

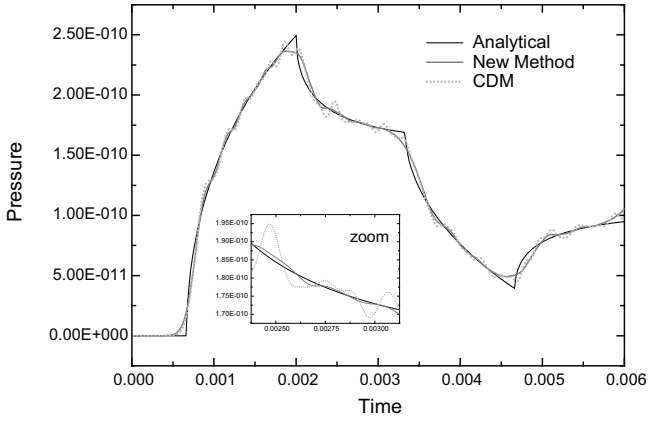

(a) discretization 1

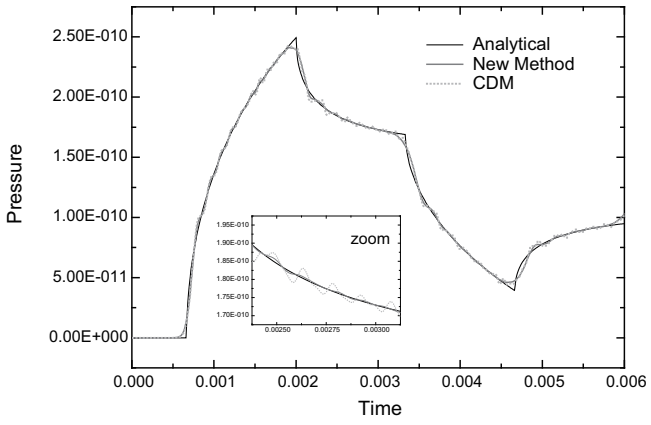

(b) discretization 2

Figure 16: Time history results at the middle of the fluid layer considering different procedures.

In Figs.14 and 15, the influence of the a parameter is analyzed. In Fig.14, results at $t = 0.006s$ are depicted, considering the new technique and different values for a. In Fig.15, the elements with non-unitary α values are marked, at $t = 0.006s$. As

one can observe in Fig. 14, relatively good results are obtained considering $a > 0$, even if low a values are selected. This is the case since the method automatically adapts itself, generating more dissipative elements (see Fig.15) once the dissipative capacity of the elements is reduced (i.e., once lower a values are considered). Thus, the adaptive method is quite robust, properly eliminating spurious modes independently of the input data.

In Fig.16, time history results for the computed hydrodynamic pressure at the middle of the fluid layer are depicted, taking into account the aforementioned procedures and discretizations. In Tab.1, the computed relative errors are provided, once again indicating the better performance of the new technique.

5 Conclusions

An adaptive time marching technique is discussed here to analyze hyperbolic problems. The technique is conditionally stable ($\Omega_c = 2\alpha^{-1/2}$), second-order accurate and it allows spurious high frequency modes to be properly dissipated, barely damaging the accuracy of the lower modes solution. The algorithm dissipative features are locally and adaptively calculated, taking into account the evolution of the computed solution. Thus, a more effective time marching technique arises, enabling enhanced dissipation and accuracy characteristics. Here, dissipative elements are activated or not, based on a simple oscillatory criterion (equation (7)), which is evaluated at each time step. The intensity of the numerical damping that is introduced into the active dissipative elements is controlled by the a parameter ($a \geq 0$), and the main features of the central difference method are reproduced when $a = 0$.

The proposed technique is simple and easy to implement. Moreover, as described in section 2, the method is truly self-starting, requiring no initial procedures at all. Thus, even by always adopting $\alpha = 1$ (i.e., no dissipative properties), the proposed technique may be considered better than the nearly universally used central difference method, due to its simplicity and self-starting attribute. In sections 3 and 4, numerical results are presented, illustrating the good performance of the methodology. As it is discussed in section 4, the new technique is robust and accurate, very properly providing explicit solutions for complex problems.

Acknowledgement: The financial support by CNPq (*Conselho Nacional de Desenvolvimento Científico e Tecnológico*) and FAPEMIG (*Fundação de Amparo à Pesquisa do Estado de Minas Gerais*) is greatly acknowledged.

References

Bathe, K. J. (1996): *Finite Element Procedures*. Prentice-Hall, Englewood Cliffs,

NJ.

Cho, J. Y.; Kim, S. J. (2002): An explicit discontinuous time integration method for dynamic-contact/impact problems. *CMES: Computer Modeling in Engineering & Sciences*, vol. 3, pp. 687–698.

Choi, C. K.; Chung, H. J. (1996): Error estimates and adaptive time stepping for various direct time integration methods. *Computers & Structures*, vol. 60, pp. 923–944.

Clough, R. W.; Penzien, J. (1993): *Dynamics of Structures*, second ed. McGraw-Hill, New York.

Gravouil, A.; Combescure, A. (2001): Multi-time-step explicit–implicit method for non-linear structural dynamics. *International Journal for Numerical Methods in Engineering*, vol. 50, pp. 199–225.

Hilber, H. M.; Hughes, T. J. R.; Taylor, R. L. (1977): Improved numerical dissipation for time integration algorithms in structural dynamics. *Earthquake Engineering and Structural Dynamics*, vol. 5, pp. 283–292.

Hughes, T. J. R. (2000): *The Finite Element Method*. Dover Publications INC, New York.

Hulbert, G. M.; Chung, J. (1996): Explicit time integration algorithms for structural dynamics with optimal numerical dissipation. *Computer Methods in Applied Mechanics and Engineering*, vol. 137, pp. 175–188.

Idesman, A. (2011): Accurate time integration of linear elastodynamics problems. *CMES: Computer Modeling in Engineering & Sciences*, vol. 71, pp. 111–148.

Lages, E. N.; Silveira, E. S. S.; Cintra, D. T.; Frery, A. C. (2013): An adaptive time integration strategy based on displacement history curvature. *International Journal for Numerical Methods in Engineering*, vol. 93, pp. 1235–1254.

Leontyev, V. A. (2010): Direct time integration algorithm with controllable numerical dissipation for structural dynamics: two-step Lambda method. *Applied Numerical Mathematics*, vol. 60, pp. 277–292.

Logg, A. (2004): Multi-Adaptive Time-Integration. *Applied Numerical Mathematics*, vol. 48, pp. 339-354.

Mansur, W. J.; Loureiro, F. S.; Soares, D.; Dors, C. (2007): Explicit time domain approaches based on numerical Green's functions computed by finite differences: the ExGA family. *Journal of Computational Physics*, vol. 227, pp. 851–870.

Miranda, I.; Ferencz, R. M.; Hughes, T. J. R. (1989): An improved implicit-explicit time integration method for structural dynamics. *Earthquake Engineering and Structural Dynamics*, vol. 18, pp. 643-653.

Rossi, D. F.; Ferreira, W. G.; Mansur, W. J.; Calenzani, A. F. G. (2014): A review of automatic time-stepping strategies on numerical time integration for structural dynamics analysis. *Engineering Structures*, vol. 80, pp. 118–136.

Soares, D. (2011): A new family of time marching procedures based on Green's function matrices. *Computers & Structures*, vol. 89, pp. 266–276.

Soares, D. (2014): An explicit family of time marching procedures with adaptive dissipation control. *International Journal for Numerical Methods in Engineering*, vol. 100, pp. 165–182.

Soares, D. (2015a): A simple and effective new family of time marching procedures for dynamics. *Computer Methods in Applied Mechanics and Engineering*, vol. 283, pp. 1138–1166.

Soares, D. (2015b): A second-order time-marching procedure with enhanced accuracy. *CMES: Computer Modeling in Engineering & Sciences*, vol. 105, pp. 341–360.